THE POG TECHNIQUE FOR MODELLING MULTI-PHASE PERMANENT MAGNET SYNCHRONOUS MOTORS

Roberto Zanasi[1]**, Federica Grossi**[1]

[1]DII, University of Modena and Reggio Emilia
Via Vignolese 905, 41100 Modena, Italy

roberto.zanasi@unimore.it(Roberto Zanasi)

Abstract

In the paper the Power-Oriented Graphs (POG) technique is used for modelling n-phase permanent magnet synchronous motors. The POG technique is a graphical modelling technique which uses only two basic blocks (the "elaboration" and "connection" blocks) for modelling physical systems. Its main characteristics are the following: it keeps a direct correspondence between pairs of system variables and real power flows; the POG blocks represent real parts of the system; it is suitable for representing physical systems both in scalar and vectorial fashion; the POG schemes can be easily transformed, both graphically and mathematically; the POG schemes are simple, modular, easy to use and suitable for education. The POG model of the considered electrical motor shows very well, from a "power" point of view, its internal structure: the electric part of the motor interacts with the mechanical part by means of a "connection" block which neither store nor dissipate energy. The dynamic model of the motor is as general as possible and it considers an arbitrary odd number of phases and an arbitrary number of harmonics of the rotor flux waveform. Generalized orthonormal transformations allow to write the dynamic equations of the system in a very compact way. The model is finally implemented with Matlab/Simulink software. The Simulink structure of the motor clearly reflects its POG representation. Simulation results are then presented to validate the machine model.

Keywords: Modelling, Simulation, multi-phase synchronous motors, arbitrary rotor flux, Graphical modelling techniques, Power-Oriented Graphs.

Presenting Author's Biography

Roberto Zanasi. He graduated with honors in Electrical Engineering in 1986. Since 1998 he has been working as Associate Professor of Automatic Control at University of Modena and Reggio Emilia. In 2004 he became Professor in Automatic Control. He held the position of Visiting Scientist at the IRIMS of Moscow in 1991, at the MIT of Boston in 1992 and at the Universit Catholique de Louvain in 1995. His research interests include: mathematical modelling, simulation, automotive, control of variable-structure systems, integral control, robotics, etc.

1 Introduction

A well known graphical technique for modelling physical systems is the *Bond Graphs* technique, see [1], [2] and the references therein. This modelling technique uses power interaction between systems as the basic concept for modelling. It has also a formal graphical language to represent the basic components that may appear in a broad range of physical systems. However this technique has few drawbacks: the graphical schematic representation needs more than 10 symbols to represent physical systems and it is not easily readable; the "power" variables must be classified in "effort" and "flow" variables and finally the implementation of the bond graphs on a general purpose computer simulator may require a non trivial "translation" (causality problem).

As for *Bond Graphs*, the basic idea of the *Power-Oriented Graphs* (POG) modelling technique is to use the power interaction between subsystems as basic concept for modelling. Please refer to [3], [4] and [5] for further details. This approach allows the modelling of a wide variety of systems involving different energetic domains. Differently from the bond graphs technique, the POG modelling technique uses only three basic symbols, it does not need to classify the power variables and it solves directly the causality problem. By this way, the POG schemes are easily readable, close to the computer implementation and allow reliable simulations using every computer simulator. A list of references of examples of application of the POG technique can be found in [6].

The paper is organized in the following way. Section 2 states the basic properties of the POG modelling technique. Section 3 shows the details of POG modelling of n-phase permanent magnet synchronous motors. Finally, in Section 4 some simulations are reported.

1.1 Notations

In the paper the following notations will be used:
- Row matrices:

$$\llbracket R_i \rrbracket_{1:n}^{i} = [\begin{array}{cccc} R_1 & R_2 & \ldots & R_n \end{array}]$$

- Column and diagonal matrices:

$$\llbracket R_i \rrbracket_{1:n}^{i} = \begin{bmatrix} R_1 \\ R_2 \\ \vdots \\ R_n \end{bmatrix}, \qquad \llbracket R_i \rrbracket_{1:n}^{i} = \begin{bmatrix} R_1 & & & \\ & R_2 & & \\ & & \ddots & \\ & & & R_n \end{bmatrix}$$

- Full matrices:

$$\llbracket R_{i,j} \rrbracket_{1:n\ 1:m}^{i\ \ j} = \begin{bmatrix} R_{11} & R_{12} & \cdots & R_{1m} \\ R_{21} & R_{22} & \cdots & R_{2m} \\ \vdots & \vdots & \ddots & \vdots \\ R_{n1} & R_{n2} & \cdots & R_{nm} \end{bmatrix}$$

- The symbol

$$\sum_{n=a:d}^{b} c_n = c_a + c_{a+d} + c_{a+2d} + c_{a+3d} + ...$$

will be used for representing the sum of a succession of numbers c_n where the index n ranges from a to b with increment d that is, using the Matlab symbology, $n = [a : d : b]$.
- The symbol $\lfloor x \rfloor$ will be used for denoting the integer part of x rounded towards below.
- The symbol $\mathbf{I}_m$ will be used for denoting the identity matrix of order m.
- Function $\mod(\theta, 2\pi)$ is the remainder of variable θ after division by coefficient 2π.

2 The bases of Power-Oriented Graphs

The "Power-Oriented Graphs" are "signal flow graphs" combined with a particular "modular" structure essentially based on the two blocks shown in Fig. 1. The basic characteristic of this modular structure is the direct correspondence between pairs of system variables and real power flows: the product of the two variables involved in each dashed line of the graph has the physical meaning of "power flowing through the section". The
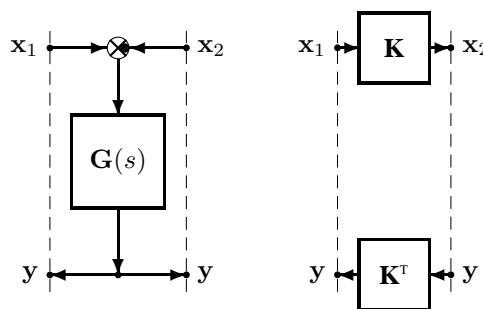

Fig. 1 Basic blocks: elaboration block (e.b.) and connection block (c.b.).

two basic blocks shown in Fig. 1 are named "elaboration block" (e.b.) and "connection block" (c.b.). The circle present in the e.b. is a summation element and the black spot represents a minus sign that multiplies the entering variable. There is no restriction on $\mathbf{x}$ and $\mathbf{y}$ other than the fact that the inner product $\langle \mathbf{x}, \mathbf{y} \rangle = \mathbf{x}^{\mathsf{T}}\mathbf{y}$ must have the physical meaning of a "power".

The e.b. and the c.b. are suitable for representing both scalar and vectorial systems. In the vectorial case, $\mathbf{G}(s)$ and $\mathbf{K}$ are matrices: $\mathbf{G}(s)$ is always square, $\mathbf{K}$ can also be rectangular. While the elaboration block can store and dissipate energy (i.e. springs, masses and dampers), the connection block can only "transform" the energy, that is, transform the system variables from one type of energy-field to another (i.e. any type of gear reduction). In the linear vectorial case when $\mathbf{G}(s) = [\mathbf{M}s + \mathbf{R}]^{-1}$, ($\mathbf{M}$ is symmetric and positive definite) the energy E_s stored in the e.b. and the power P_d dissipating in the e.b. can be expressed as:

$$E_s = \frac{1}{2}\mathbf{y}^{\mathsf{T}}\mathbf{M}\,\mathbf{y}, \qquad P_d = \mathbf{y}^{\mathsf{T}}\mathbf{R}\,\mathbf{y}$$

There is a direct correspondence between POG representations and the corresponding state space descrip-

tions. For example, the system

$$\begin{cases} \mathbf{L\,\dot{x}} &= \mathbf{Ax + Bu} \\ \mathbf{y} &= \mathbf{B^{\scriptscriptstyle T} x} \end{cases} \qquad \mathbf{L = L^{\scriptscriptstyle T} > 0} \qquad (1)$$

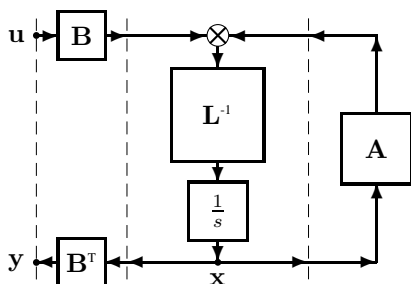can be represented by the POG scheme shown in Fig. 2.

Fig. 2 POG block scheme of a generic dynamic system.

When an eigenvalue of matrix $\mathbf{L}$ tends to zero (or to infinity), system (1) degenerates towards a lower dimension dynamic system. In this case, the dynamic model of the "reduced" system can be directly obtained from (1) by using a simple "congruent" transformation $\mathbf{x = Tz}$ ($\mathbf{T}$ is constant):

$$\begin{cases} \mathbf{T^{\scriptscriptstyle T}LT\dot{z} = T^{\scriptscriptstyle T}ATz + T^{\scriptscriptstyle T}Bu} \\ \mathbf{y = B^{\scriptscriptstyle T}Tz} \end{cases} \Leftrightarrow \begin{cases} \overline{\mathbf{L}}\dot{\mathbf{z}} = \overline{\mathbf{A}}\mathbf{z} + \overline{\mathbf{B}}\mathbf{u} \\ \mathbf{y} = \overline{\mathbf{B}}^{\scriptscriptstyle T}\mathbf{z} \end{cases}$$

where $\overline{\mathbf{L}} = \mathbf{T^{\scriptscriptstyle T}LT}$, $\overline{\mathbf{A}} = \mathbf{T^{\scriptscriptstyle T}AT}$ and $\overline{\mathbf{B}} = \mathbf{T^{\scriptscriptstyle T}B}$. If matrix $\mathbf{T}$ is time-varying, an additional term $\mathbf{T^{\scriptscriptstyle T}L\dot{T}z}$ appears in the transformed system. When matrix $\mathbf{T}$ is rectangular, the system is transformed and reduced at the same time.

3   Electrical motors modelling

In this paper we will refer only to permanent magnet synchronous electrical motors with an *odd* number of phases. In Fig. 3 it is shown the electromechanical structure of a five-phase motor in the case of single polar expansion ($p = 1$). The considered multi-phase electrical motor is characterized by the following parameters:
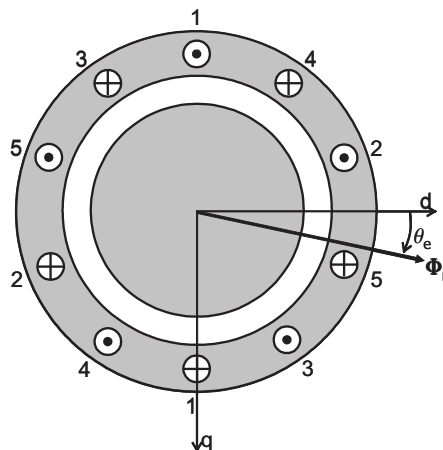

Fig. 3 Structure of a five-phase motor in the case of single polar expansion ($p = 1$)

m	: number of motor phases;
p	: number of polar expansions;
θ_r	: rotor angular position;
ω_r	: rotor angular speed;
θ	: electric angle: $\theta = p\,\theta_r$;
N_c	: number of coils for each phase;
R_i	: i-th phase resistance ($p = 1$);
L_i	: i-th phase self induction coefficient ($p = 1$);
M_{ij}	: mutual induction coefficient of i-th phase coupled with j-th phase ($p = 1$);
$\phi(\theta)$	: rotor permanent magnet flux;
$\phi_c(\theta)$	: total rotor flux chained with stator phase 1;
$\phi_{ci}(\theta)$	: total rotor flux chained with stator phase i-th;
φ_r	: maximum value of function $\phi(\theta)$;
φ_c	: maximum value of function $\phi_c(\theta)$;
J_r	: rotor inertia momentum;
b_r	: rotor linear friction coefficient;
τ_r	: electromotive torque acting on the rotor;
τ_e	: external load torque acting on the rotor;
γ	: basic angular displacement;

Fluxes $\phi(\theta)$ and $\phi_c(\theta)$ satisfy relations:

$$\phi_c(\theta) = p\,N_c\,\phi(\theta) = p\,N_c\,\varphi_r\,\bar{\phi}(\theta) = \varphi_c\,\bar{\phi}(\theta)$$

where $\varphi_c = p\,N_c\,\varphi_r$ and $\bar{\phi}(\theta)$ is the rotor flux function normalized respectively to its maximum value φ_r.

Let $\gamma = \frac{2\pi}{m}$ denote the basic angular phase displacement for electrical motors with m phases. Referring to the considered multi-phase electrical motor, the following hypotheses are assumed:

H1) Function $\phi(\theta)$ is periodic with period 2π;
H2) Function $\phi(\theta)$ is an even function of θ;
H3) Function $\phi(\theta + \frac{\pi}{2})$ is an odd function of θ;
H4) For $\theta = 0$ the rotor flux $\phi_c(\theta)$ chained with phase 1 is maximum;
H5) The electrical motor is homogeneous in its electrical characteristics.

The electrical coupling of a generic couple of phases i and j of the motor is shown Fig. 4. The differential equation describing the dynamic behaviour of the i-th
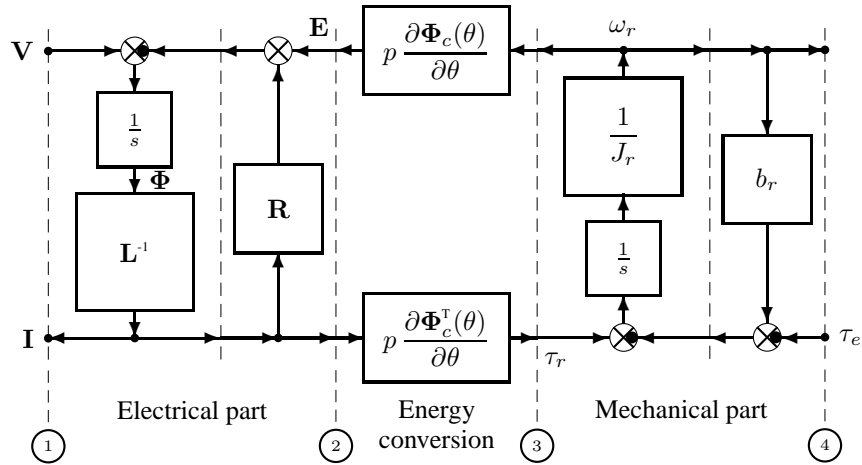
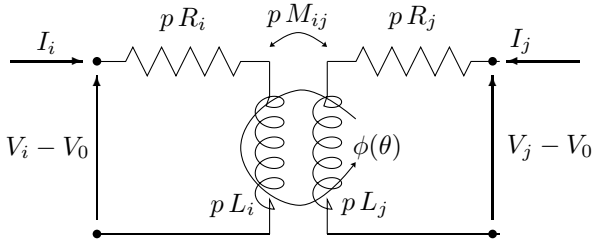Fig. 5 POG scheme of the multi-phase motor dynamic model.

Fig. 4 Electric coupling of a generic couple of phases i and j of the motor.

phase of the motor is the following:

$$\frac{d\tilde{\phi}_{ci}}{dt} = V_i - V_0 - p\,R_i I_i, \qquad i = 1, \ldots, m \quad (2)$$

where $V_i - V_0$ is the voltage applied to the i-th phase and $\tilde{\phi}_{ci}$ is the total magnetic flux chained with the i-th phase:

$$\tilde{\phi}_{ci} = p\,L_i I_i + p \sum_{j=1,\, j \neq i}^{m} M_{ij} I_j + \phi_{ci}(\theta). \quad (3)$$

V_0 represents the reference common voltage for all the phases. If the m phases are star-connected it can be shown that V_0 is the voltage at the star centre and $V_0 = \frac{1}{m}\sum_{i=1}^{m} V_i$. However, when the system is star-connected the input voltages V_i are defined with a degree of freedom, so without loss of generality in (2) one can set $V_0 = 0$. If the m phases are independent, V_0 is the ground voltage and in this case too one can set $V_0 = 0$. Let's introduce the vectors:

$$\mathbf{I} = \begin{bmatrix} I_1 \\ I_2 \\ \vdots \\ I_m \end{bmatrix}, \qquad \mathbf{V} = \begin{bmatrix} V_1 \\ V_2 \\ \vdots \\ V_m \end{bmatrix}$$

and let's indicate with $\mathbf{\Phi}_c(\theta)$ the vector of chained rotor fluxes. Due to the magnetic symmetry of the electrical

motor (see H5) we have that:

$$\mathbf{\Phi}_c(\theta) = \begin{bmatrix} \phi_{c1}(\theta) \\ \phi_{c2}(\theta) \\ \vdots \\ \phi_{cm}(\theta) \end{bmatrix} = \begin{bmatrix} \phi_c(\theta) \\ \phi_c(\theta - \gamma) \\ \phi_c(\theta - 2\gamma) \\ \vdots \\ \phi_c(\theta - (m-1)\gamma) \end{bmatrix}. \quad (4)$$

Let $\tilde{\mathbf{\Phi}}_c$ denote the vector of "chained total magnetic fluxes" defined in (3):

$$\tilde{\mathbf{\Phi}}_c(\mathbf{I}, \theta) = \mathbf{L}\,\mathbf{I} + \mathbf{\Phi}_c(\theta) \quad (5)$$

where $\mathbf{L} > 0$ is the following positive-definite symmetric matrix:

$$\mathbf{L} = p \begin{bmatrix} L_1 & M_{12} & M_{13} & \cdots & M_{1m} \\ M_{12} & L_2 & M_{23} & \cdots & M_{2m} \\ M_{13} & M_{23} & L_3 & \cdots & M_{3m} \\ \vdots & \vdots & & \ddots & \vdots \\ M_{1m} & M_{2m} & M_{3m} & \cdots & L_m \end{bmatrix}.$$

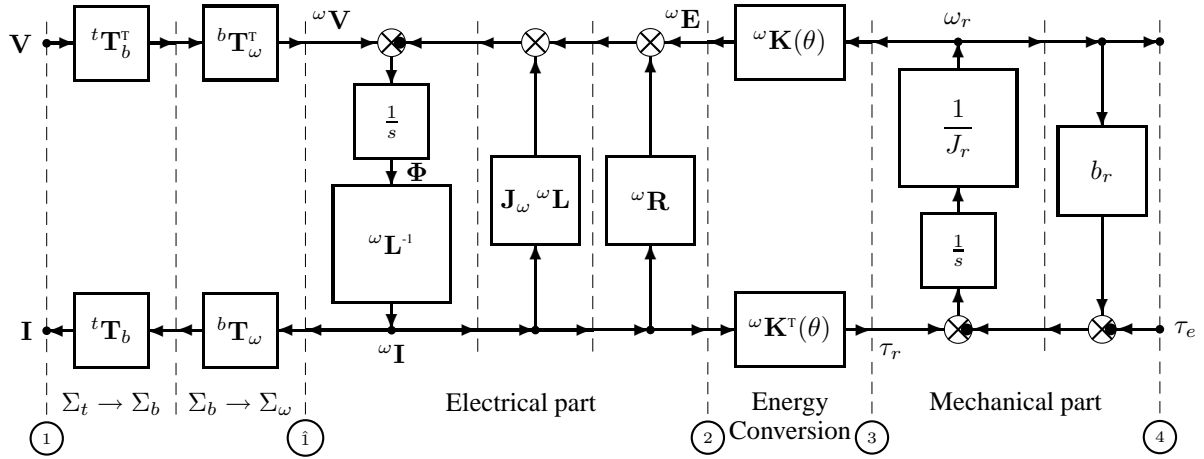The system of m differential equations (2) can be rewritten in matrix form as:

$$\frac{d\tilde{\mathbf{\Phi}}_c(\mathbf{I}, \theta)}{dt} = \mathbf{V} - \mathbf{R}\,\mathbf{I} \quad (6)$$

where $\mathbf{R}$ is the diagonal matrix:

$$\mathbf{R} = p \overset{i}{\underset{1:m}{[\![}} R_i \,{]\!]}.$$

From Eqs. (4) and (5) we have that:

$$\frac{d(\mathbf{L}\,\mathbf{I})}{dt} = \mathbf{V} - \mathbf{R}\mathbf{I} - \overbrace{\underbrace{p\,\frac{\partial\mathbf{\Phi}_c(\theta)}{\partial\theta}}_{\mathbf{K}_\tau(\theta)}\,\omega_r}^{\mathbf{E}} \quad (7)$$

Fig. 6 POG scheme of a multi-phase electrical motor in the transformed space Σ_ω.

where $\mathbf{K}_\tau(\theta) = p\frac{\partial \mathbf{\Phi}_c(\theta)}{\partial \theta}$ is the vector that multiplied by ω_r gives the counter-electromotive forces $\mathbf{E} = \mathbf{K}_\tau(\theta)\omega$ acting on the electrical part of the motor. The differential equation describing the mechanical part of the motor is:

$$\frac{d(J_r\omega_r)}{dt} = \tau_r - \tau_e - b_r\,\omega_r. \qquad (8)$$

Since the energy $E(\mathbf{I}, \omega_r, \theta_r)$ stored in the electromechanical system is:

$$E(\mathbf{I}, \omega_r, \theta_r) = \frac{1}{2}\mathbf{I}^{\mathrm{T}}\mathbf{L}\mathbf{I} + \int_0^{\mathbf{\Phi}_c(p\theta_r)} \mathbf{I}^{\mathrm{T}}\,d\mathbf{\Phi}_c(p\theta_r) + \frac{1}{2}J_r\omega_r^2$$

the electromotive torque can be calculated as follows:

$$\tau_r = \frac{\partial E(\mathbf{I}, \omega_r, \theta_r)}{\partial \theta_r} = \underbrace{p\frac{\partial \mathbf{\Phi}_c^{\mathrm{T}}(\theta)}{\partial \theta}}_{\mathbf{K}_\tau^{\mathrm{T}}(\theta)}\mathbf{I} = \mathbf{K}_\tau^{\mathrm{T}}(\theta)\,\mathbf{I}.$$

Relations (7) and (8) can be graphically represented by the POG scheme shown in Fig. 5. The elaboration blocks present between the power sections ① and ② represent the *Electrical part* of the system, while the blocks between sections ③ and ④ represent the *Mechanical part* of the system. The connection block present between sections ② and ③ represents the conversion of energy and powers (without accumulation nor dissipation) between the electrical and mechanical domains. Function $\phi_c(\theta)$ is even and periodic of period 2π so it can be developed in Fourier series of cosines with only odd harmonics:

$$\phi_c(\theta) = \varphi_c\,\bar{\phi}(\theta) = \varphi_c\sum_{n=1:2}^{\infty} a_n\cos(n\theta). \qquad (9)$$

From (4) and (9) it follows that vector $\mathbf{\Phi}_c(\theta)$ can be rewritten in a compact form as:

$$\mathbf{\Phi}_c(\theta) = \varphi_c\left\|\left[\sum_{n=1:2}^{\infty} a_n\cos[n(\theta - h\,\gamma)]\right]\right\|_{0:m-1}. \qquad (10)$$

From (7) and (10) one obtains vector $\mathbf{K}_\tau(\theta)$:

$$\mathbf{K}_\tau(\theta) = p\,\varphi_c\left\|\left[-\sum_{n=1:2}^{\infty} n\,a_n\sin[n(\theta - h\,\gamma)]\right]\right\|_{0:m-1}. \qquad (11)$$

Let us now consider the two following orthonormal transformations:

$$^t\mathbf{T}_b = \sqrt{\frac{2}{m}}\left[\left\|\left[\cos(hk\gamma),\ -\sin(hk\gamma)\right]\right\|_{\substack{0:m-1\\1:2:m-2}},\ \left\|\left[\frac{1}{\sqrt{2}}\right]\right\|_{0:m-1}\right]$$

$$^b\mathbf{T}_\omega = \left[\begin{array}{cc} \left\|\left[\begin{array}{cc}\cos(k\theta) & \sin(k\theta)\\ -\sin(k\theta) & \cos(k\theta)\end{array}\right]\right\|_{1:2:m-2} & , 0\\ 0 & , 1\end{array}\right].$$

Matrix $^t\mathbf{T}_b$ is similar to the generalized Concordia transformation but with a permutation on columns. This matrix transforms the system variables from the original reference frame Σ_t to an intermediate reference frame Σ_b. Matrix $^b\mathbf{T}_\omega$ represents a multiple rotation in the state space as function of the electrical motor angle θ. This matrix transforms the system from the intermediate reference frame Σ_b to final rotating reference frame Σ_ω. The product of these two matrices $^t\mathbf{T}_\omega = {}^t\mathbf{T}_b\,{}^b\mathbf{T}_\omega$ is still an orthonormal transformation, from Σ_t to Σ_ω, with the following structure:

$$^t\mathbf{T}_\omega^{\mathrm{T}} = {}^\omega\mathbf{T}_t = \sqrt{\frac{2}{m}}\left[\begin{array}{c}\left\|\left[\begin{array}{c}\cos(k\,(\theta - h\,\gamma))\\ \sin(k\,(\theta - h\,\gamma))\end{array}\right]\right\|_{\substack{1:2:m-2\\0:m-1}}\\ \left\|\left[\frac{1}{\sqrt{2}}\right]\right\|_{0:m-1}\end{array}\right].$$

Since the multi-phase motor is homogeneous in its elec-

trical characteristics, see hypothesis H5, we can set

$$\begin{cases} M_{ij} = M_0 \cos((i-j)\gamma) \\ L_i = \Delta_0 + M_0 \\ R_i = R \end{cases} \quad i,j \in \{1,2,...,m\}$$

where Δ_0 and M_0 are proper parameters characterizing the self and mutual induction coefficients of the motor phases. Applying transformation ${}^t\mathbf{T}_\omega$ to matrices $\mathbf{L}$, $\mathbf{R}$ and $\mathbf{K}_\tau(\theta)$ one obtains the following transformed matrices ${}^\omega\mathbf{L} = {}^\omega\mathbf{T}_t\, \mathbf{L}\, {}^t\mathbf{T}_\omega$, ${}^\omega\mathbf{R}$ and ${}^\omega\mathbf{K}_\tau(\theta)$:

$${}^\omega\mathbf{L} = p \begin{bmatrix} \Delta_0 + \frac{mM_0}{2} & 0 & 0 & 0 & \cdots & 0 \\ 0 & \Delta_0 + \frac{mM_0}{2} & 0 & 0 & \cdots & 0 \\ 0 & 0 & \Delta_0 & 0 & \cdots & 0 \\ 0 & 0 & 0 & \Delta_0 & \cdots & 0 \\ \vdots & \vdots & \vdots & \vdots & \ddots & \vdots \\ 0 & 0 & 0 & 0 & \cdots & \Delta_0 \end{bmatrix},$$

$${}^\omega\mathbf{R} = {}^\omega\mathbf{T}_t\,\mathbf{R}\,{}^t\mathbf{T}_\omega = \mathbf{R} = p\,R\,\mathbf{I}_m,$$

$${}^\omega\mathbf{K}_\tau(\theta) = {}^\omega\mathbf{T}_t\,\mathbf{K}_\tau(\theta) = -p\,\varphi_c\sqrt{\frac{m}{2}}\cdot$$

$$\cdot \begin{bmatrix} \begin{bmatrix} \sum_{n=0:2m}^\infty [(n+k)\,a_{n+k}+(n-k)\,a_{n-k}]\sin(n\theta) \\ \sum_{n=0:2m}^\infty [(n+k)\,a_{n+k}-(n-k)\,a_{n-k}]\cos(n\theta) \end{bmatrix}_{1:2:m-2} \\ -\sqrt{2}\sum_{n=m:2m}^\infty n a_n \sin(n\theta) \end{bmatrix} \quad (12)$$

Note that vector ${}^\omega\mathbf{K}_\tau(\theta)$ is composed only by harmonics $\sin(n\theta)$ and $\cos(n\theta)$ where n is an integer number multiple of $2m$. Moreover, vector ${}^\omega\mathbf{K}_\tau$ can be easily computed knowing the coefficients a_n of the Fourier series of the rotor flux, see Eq. (9).

In the transformed space Σ_ω, the dynamic equations of the multi-phase electrical motor (both mechanical and electrical parts) can be represented in compact form as:

$$\begin{bmatrix} {}^\omega\mathbf{L} & 0 \\ 0 & J_r \end{bmatrix}\begin{bmatrix} {}^\omega\dot{\mathbf{I}} \\ \dot{\omega}_r \end{bmatrix} = -\begin{bmatrix} {}^\omega\mathbf{R}+\mathbf{J}_\omega\,{}^\omega\mathbf{L} & {}^\omega\mathbf{K}_\tau \\ -{}^\omega\mathbf{K}_\tau^\mathsf{T} & b_r \end{bmatrix}\begin{bmatrix} {}^\omega\mathbf{I} \\ \omega_r \end{bmatrix}+\begin{bmatrix} {}^\omega\mathbf{V} \\ -\tau_e \end{bmatrix}$$
(13)

where ${}^\omega\mathbf{I} = {}^\omega\mathbf{T}_t\,\mathbf{I}$, ${}^\omega\mathbf{V} = {}^\omega\mathbf{T}_t\,\mathbf{V}$ and matrix $\mathbf{J}_\omega$ is:

$$\mathbf{J}_\omega = \begin{bmatrix} \begin{bmatrix} 0 & -k\omega_e \\ k\omega_e & 0 \end{bmatrix}_{1:2:m-2} & 0 \\ 0 & 1 \end{bmatrix}.$$

If the m phases of the rotor are star-connected then $\sum_{i=1}^m I_i = 0$ and so ${}^\omega I_m = 0$. In this case the m-th equation of system (13) is a static relation that can be eliminated letting the system reduce to order $m-1$.

The POG scheme describing the considered multi-phase electrical motor in the transformed space Σ_ω is

shown in Fig. 6. Note that the POG scheme is easy to read, it clearly shows the sections where powers flow (the thin dashed lines) and it has a direct correspondence with the state space description (13). Moreover, this POG scheme can be directly introduced (more or less "as it is") and simulated in Simulink.

3.1 Fourier series of the rotor flux

The Fourier series of some periodic rotor fluxes of practical interest are listed below.
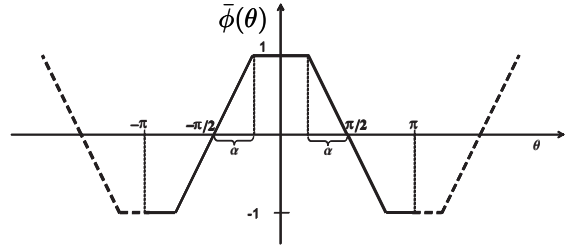
- *Trapezoidal waveform*, see Fig. 8:

Fig. 8 Trapezoidal waveform $\bar{\phi}(\theta)$ with $0 \le \alpha \le \frac{\pi}{2}$.

$$\bar{\phi}(\theta) = \frac{4}{\pi}\sum_{n=1:2}^\infty \sin\left(n\frac{\pi}{2}\right)\frac{\sin(n\alpha)}{\alpha\,n^2}\cos(n\theta). \quad (14)$$

The Fourier series of the *Square* and *Triangular waveforms* can be easily obtained from (14) by setting, respectively, $\alpha = 0$ and $\alpha = \frac{\pi}{2}$.

- *Cosinusoidal interpolatated waveform.* The signal $\phi(\theta)$ shown in Fig.9 is defined as follows:
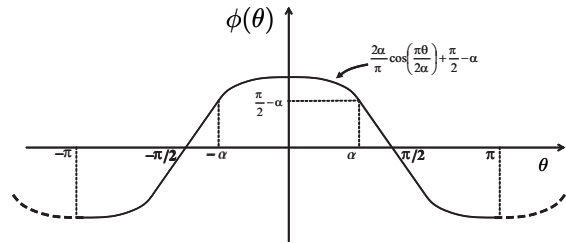

Fig. 9 Cosinusoidal interpolatated waveform $\phi(\theta)$.

$$\phi(\theta) = \begin{cases} \frac{2\alpha}{\pi}\cos\left(\frac{\pi\theta}{2\alpha}\right) + \frac{\pi}{2} - \alpha, & \theta \in [0,\alpha] \\ -\theta, & \theta \in \left[\alpha,\frac{\pi}{2}\right] \end{cases}$$

Its Fourier series is:

$$\phi(\theta) = \sum_{n=1:2}^\infty \frac{4\pi\cos(n\alpha)}{n^2(\pi^2 - 4n^2\alpha^2)}\cos(n\theta).$$

The normalized function is:

$$\bar{\phi}(\theta) = \frac{\phi(\theta)}{\left(\frac{2\alpha}{\pi} + \frac{\pi}{2} - \alpha\right)}. \quad (15)$$

- *Odd polynomial interpolation.* Let us consider the family of periodic signals $\bar{\phi}(r,\theta)$ shown in Fig.10

$$b_n(r) = \frac{4\prod\limits_{j=1}^{\frac{r-1}{2}}(1+2j)}{\alpha^r\,\pi\,n^{r+1}}\left\{\left[\sum_{i=0}^{\left\lfloor\frac{r}{4}\right\rfloor}(-1)^i\binom{\frac{r-1}{2}-i}{i}(\alpha n)^{2i}\prod_{j=i}^{\frac{r-3}{2}-i}(1+2j)\right]\sin(\alpha n)+\right.$$
$$\left.+\left[\sum_{i=0}^{\left\lfloor\frac{r}{4}\right\rfloor}(-1)^{i+1}\binom{\frac{r-1}{2}-i-1}{i}(\alpha n)^{2i+1}\prod_{j=i+1}^{\frac{r-3}{2}-i}(1+2j)\right]\cos(\alpha n)\right\}$$

Fig. 7 General formula for computing coefficients $b_n(r)$ of Fourier series of signals $\bar{\phi}(r,\theta)$.
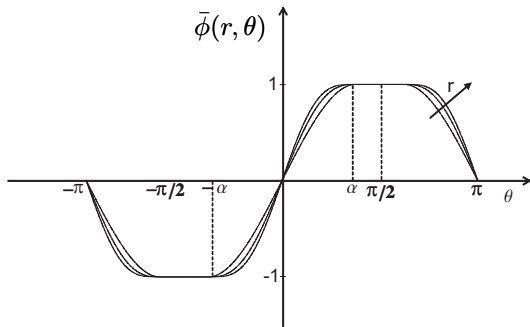
Fig. 10 Periodic signals $\bar{\phi}(r,\theta)$ for $r = 3, 5, 7$.

$$\bar{\phi}(r,\theta) = \begin{cases} \tilde{\phi}(r,\theta), & \theta \in [0,\alpha] \\ 1, & \theta \in \left[\alpha,\frac{\pi}{2}\right] \end{cases}$$

where $\tilde{\phi}(r,\theta)$ is a polynomial (r is odd) with the following structure:

$$\tilde{\phi}(r,\theta) = d_1(r)\theta + d_3(r)\theta^3 + ... + d_r(r)\theta^r.$$

The polynomial coefficients $d_i(r)$ can be computed, for $i \in \{1, 3, ..., r\}$, considering the following continuity conditions:

$$\begin{cases} \tilde{\phi}(r,\alpha) = 1 \\ \tilde{\phi}'(r,\alpha) = 0 \\ \vdots \\ \tilde{\phi}^{(\frac{r+1}{2})}(r,\alpha) = 0 \end{cases}$$

The Fourier series of signals $\bar{\phi}(r,\theta)$ is

$$\bar{\phi}(r,\theta) = \sum_{n=1:2}^{\infty} b_n(r)\sin(n\theta) \qquad (16)$$

where coefficients $b_n(r)$ can be calculated using the general formula reported in Fig. 7.

- *Even polynomial interpolation.* Let us consider the family of periodic signals $\phi(q,\theta)$ shown in Fig.11:

$$\phi(q,\theta) = \begin{cases} \tilde{\phi}(q,\theta), & \theta \in [0,\alpha] \\ \frac{\pi}{2} - \theta, & \theta \in \left[\alpha,\frac{\pi}{2}\right] \end{cases}$$
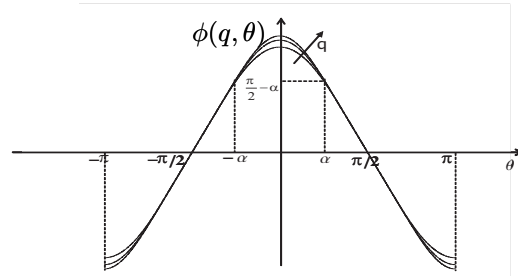

Fig. 11 Periodic signals $\phi(q,\theta)$ for $q = 2, 4, 6$.

where $\tilde{\phi}(q,\theta)$ is a polynomial (q is even) with the following structure:

$$\tilde{\phi}(q,\theta) = c_0(q) + c_2(q)\theta^2 + c_4(q)\theta^4 + ... + c_q(q)\theta^q.$$

The polynomial coefficients $c_i(q)$ can be computed, for $i \in \{0, 2, ..., q\}$, considering the following continuity conditions:

$$\begin{cases} \tilde{\phi}(q,\alpha) = \frac{\pi}{2} - \alpha \\ \tilde{\phi}'(q,\alpha) = -1 \\ \tilde{\phi}^{(j)}(q,\alpha) = 0 & \text{for} \quad j = 2, ..., \frac{q}{2} \end{cases}$$

The Fourier series of signals $\phi(q,\theta)$ is:

$$\phi(q,\theta) = \sum_{n=1:2}^{\infty} a_n(q)\cos(n\theta) \qquad (17)$$

where the series coefficients $a_n(q)$ can be obtained from the coefficients $b_n(r)$ reported in Fig. 7 as follows:

$$a_n(q) = \left.\frac{b_n(r)}{n}\right|_{r=q-1}.$$

The normalized signals

$$\bar{\phi}(q,\theta) = \frac{1}{c_0(q)}\phi(q,\theta) \qquad (18)$$

can be obtained from signals $\phi(q,\theta)$ dividing by coefficient $c_0(q)$:

$$c_0(q) = \frac{\pi}{2} - \alpha \frac{\prod\limits_{i=\left\lfloor\frac{q+2}{4}\right\rfloor}^{\frac{q-2}{2}}(2i+1)}{\left\lfloor\frac{q}{4}\right\rfloor!\,2^{\left\lfloor\frac{3q}{4}\right\rfloor}}.$$

Note that the derivative $\frac{\partial \phi(2,\theta)}{\partial \theta}$ of signal $\phi(q,\theta)$ when $q = 2$ has a trapezoidal shape and so for this type of rotor flux the counter-electromotive forces $\mathbf{E} = \mathbf{K}_\tau(\theta)\omega$ have a trapezoidal shape proportional to the motor velocity ω, see eq. (7).

4 Simulations

The POG scheme shown in Fig. 6 has been implemented in Simulink. Simulations described in this Section have been obtained using the following electrical and mechanical parameters: $m = 5$, $p = 4$, $R = 3\,\Omega$, $L_0 = 0.1$ H, $M_0 = 0.08$ H, $N_c = 100$, $N_a = 200$, $\varphi_r = 0.02$ W, $J_m = 1.6$ kg m^2, $b_m = 0.8$ Nm s/rad. Parameter N_a is the number of harmonics considered in Fourier series expansion of the rotor flux function. The simulations have been obtained with star connected phases and using for the rotor flux the cosinusoidal interpolated waveform $\bar{\phi}(\theta)$ with $\alpha = \frac{\pi}{5}$, see (15). Symmetric input voltages have been considered, it is to say:

$$V_i = V_M \cos(2\pi t + i\gamma), \qquad i \in \{0, 1, \dots, m\}$$

with $V_M = 80$ V. At time $t = 2$ s the load torque τ_e switches from 0 to 100 Nm. Figs. 12, 13 and 14 show the simulation results obtained for the following variables: phase currents $\mathbf{I}$ and $^\omega\mathbf{I}$ in the Σ_t and Σ_ω reference frames; motor angular velocity ω_r; electromotive torque τ_r; symmetric m-phases input voltages $\mathbf{V}$ and counter-electromotive voltages $^\omega\mathbf{E}$ in the transformed Σ_ω reference frame.
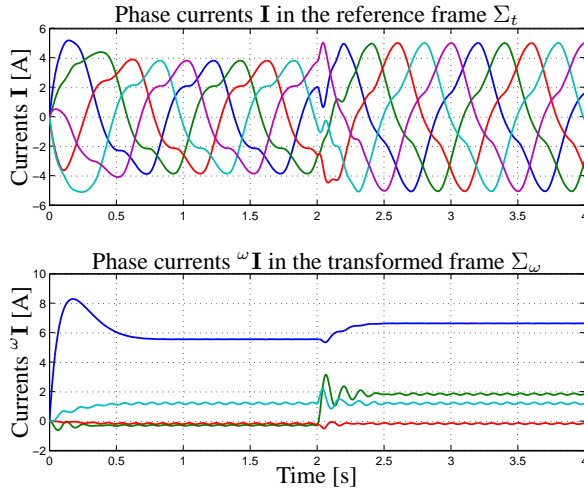

Fig. 12 Phase currents $\mathbf{I}$ and $^\omega\mathbf{I}$ in the original Σ_t and in the transformed Σ_ω reference frame respectively.

Let us now consider the control law $V_i = V_M S_i$, for $i \in \{0, 1, \dots, m\}$, where:

$$S_i = \begin{cases} 1 & \bar{\theta}_i \in [\pi + \alpha,\, 2\pi - \alpha] \\ -1 & \bar{\theta}_i \in [\alpha,\, \pi - \alpha] \\ 0 & \text{otherwise} \end{cases} \qquad (19)$$

$$\bar{\theta}_i = \mod(\theta + (i-1)\gamma, 2\pi)$$

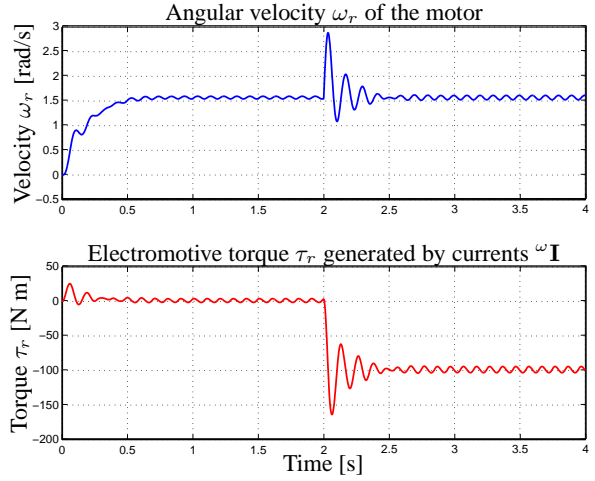This control law can be applied to the POG schemes shown in Figs. 5 and 6 by connecting at the power sec-

Fig. 13 Angular velocity ω_r of the motor and electromotive torque τ_r generated by the motor currents $^\omega\mathbf{I}$.
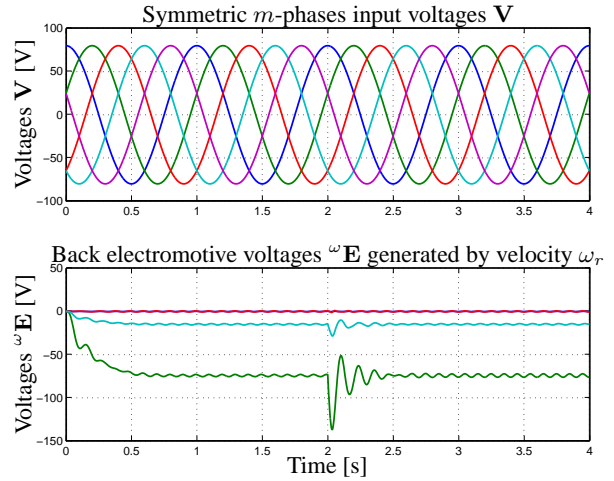

Fig. 14 Symmetric m-phases input voltages $\mathbf{V}$ and counter-electromotive voltages $^\omega\mathbf{E}$ in the transformed Σ_ω reference frame.

tion ① of these schemes the connection block shown in Fig. 15.

The simulation results shown in Figs. 16 and 17 refer to the same system parameters used in the previous simulation except for: number of polar expansion $p = 1$; the load torque is applied at time $t = 1.5$; for the rotor flux it has been chosen the normalized even polynomial interpolation function $\bar{\phi}(q, \theta)$ with $q = 2$ and $\alpha = \frac{\pi}{5}$, see (18). In this case the shape of the counter-electromotive voltages E_i is trapezoidal as it is evident in the upper part of Fig. 17. This type of control generates high torques τ_r when the angular velocity ω_r is small, see the upper part of Fig. 16 and the lower part of Fig. 17. The behaviour of the controlled system is stable with compared to the variations of the external torque τ_e, in fact the motor torque τ_r increases to face the increased external torque τ_e, see Fig. 17.
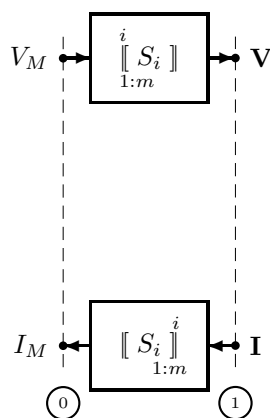
Fig. 15 POG connection block that can be used to apply the control law (19) to the POG schemes shown in Figs. 5 and 6.
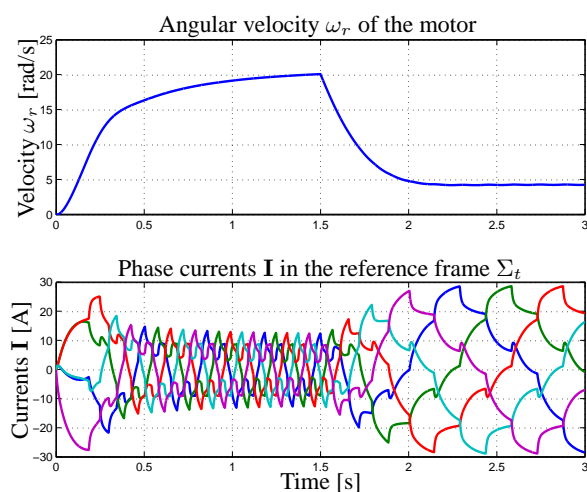

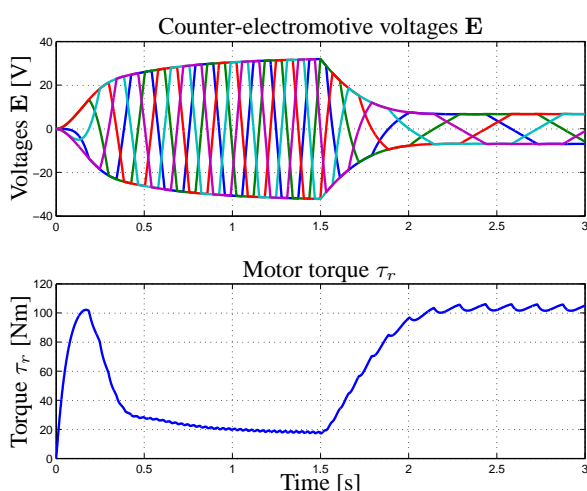Fig. 16 Angular velocity ω_r and phase currents $\mathbf{I}$ of the motor.

Fig. 17 Counter-electromotive voltages $\mathbf{E}$ and motor torque τ_r.

5 Conclusions

In this paper a n-phase permanent magnet synchronous motor has been modelled using the Power-Oriented Graphs (POG) technique. This approach exhibits some advantages in comparison with other graphical techniques and allows to realize a very compact model scheme. Moreover it can be easily translated into a Simulink model. Some simulations are carried out in order to show the effectiveness of the realized model in the case of a five-phase motor with star connection configuration. A brief list of Fourier series of the rotor flux signals has been presented and then used in the Simulink model.

6 References

[1] Paynter, H.M., *Analysis and Design of Engineering Systems*, MIT-press, Camb., MA, 1961.

[2] D. C. Karnopp, D.L. Margolis, R. C. Rosemberg, *System dynamics - Modeling and Simulation of Mechatronic Systems*, Wiley Interscience, ISBN 0-471-33301-8, 3rd ed. 2000.

[3] R. Zanasi, "Power Oriented Modelling of Dynamical System for Simulation", *IMACS Symp. on Modelling and Control of Technological System*, Lille, France, May 1991.

[4] R. Zanasi, K. Salisbury, "Dynamic Modeling, Simulation and Parameter Identification for the WAM Arm", *A.I. Memo No. 1387*, MIT, Cambridge, USA, August 1992.

[5] Zanasi R., "Dynamics of a n-links Manipulator by Using Power-Oriented Graph", *SYROCO '94*, Capri, Italy, 1994.

[6] R. Morselli, R. Zanasi, "Modeling of Automotive Control Systems Using Power Oriented Graphs", 32nd Annual Conference of the IEEE Industrial Electronics Society, IECON 2006, Parigi, 7-10 Novembre, 2006.

[7] E. Semail, X. Kestelyn, A. Bouscayrol, "Right Harmonic Spectrum for the Back-Electromotive Force of a n-phase Synchronous Motor", Industry Applications Conference, 2004, 39th IAS Annual Meeting, ISBN: 0-7803-8486-5.

[8] E. Semail, X. Kestelyn, A. Bouscayrol, "Sensitivity of a 5-phase Brushless DC machine to the 7th harmonic of the back electromotive force", 35th Annual IEEE Power Electronics Specialists Conference, 2004.